

# Crystallographic Characterization of Interconnects by Orientation Mapping in the SEM\*

C. E. Kalnas<sup>1</sup>, R. R. Keller<sup>1</sup>, and D. P. Field<sup>2</sup>

<sup>1</sup>National Institute of Standards and Technology, Materials Reliability Division, 325 Broadway, Boulder, CO 80303

<sup>2</sup>TexSEM Laboratories, 392 East 12300 South, Suite H, Draper, UT 84020

We show in this paper how electron backscatter diffraction and orientation mapping within a scanning electron microscope can be used to measure local variations in crystallographic texture and grain boundary structure in interconnects. The reliability-limiting phenomena of stress voiding and electromigration are two examples of interconnect failure modes that depend strongly on local crystallographic structure. Several analysis examples are presented to show the utility of this technique for characterization of local microstructures in both copper- and aluminum-based lines. The advantages of a local measurement technique over a global texture method for orientation determination became immediately apparent in these investigations. This local approach to characterizing crystallography is expected to play an even larger role in technologies such as damascene or lift-off processing, where lines are deposited directly into precisely-defined geometries. Particularly in these more advanced processing technologies, one cannot extrapolate measurements of blanket film structure and properties to the case of narrow lines.

## INTRODUCTION

The fact that metallizations for on-chip interconnects are fabricated with line dimensions of the order of 0.5  $\mu\text{m}$  in thickness and 0.25  $\mu\text{m}$  in width imposes stringent constraints on their reliability. Grain diameters that typically develop in physical-vapor-deposited metal films grown at relatively low temperatures are approximately as large as the film thickness (1). For interconnects with dimensions as given above, we expect the presence of single grains through the film thickness and across the line width, leading to a bamboo or near-bamboo structure. The behavior of such a material will be determined not simply by the global microstructure as inferred from blanket film characterizations, but rather by local variations in crystallographic features such as texture and grain boundary structures.

A notable example of the importance of local crystallography as opposed to global texture was demonstrated on aluminum-based interconnects by Rodbell *et al.* (2). They found that lines of stronger average texture showed shorter stress voiding lifetimes than lines of weaker average texture. This result, apparently contradictory to the conventional belief that stronger average texture results in better resistance to voiding, was clarified when measurements of local grain orientations were made. Grains adjacent to voids in the lines of stronger average texture were more randomly oriented than undamaged grains in the line. This suggested that a single off -  $\langle 111 \rangle$  grain in the strongly textured material was more detrimental than such a

grain in the weakly textured material. Such rapid changes in grain-to-grain misorientations necessarily lead to different grain boundary structures and sometimes detrimental properties in thin metal films for interconnects. A characterization method suitable for assessing interconnect microstructures at this scale is clearly necessary. Electron backscatter diffraction (EBSD) has been used successfully for making such characterizations on both aluminum and copper interconnect systems (2,3,4), revealing the significant effects of local variations in microstructure on voiding susceptibility.

EBSD in conjunction with scanning electron microscopy has been developed into a routine characterization tool over the past decade or so and has been applied to a variety of materials systems (5,6). Its very nature lends itself readily to the characterization of submicrometer metal structures such as on-chip interconnects. The scanning electron microscope (SEM) is usually operated to produce a practically monochromatic beam of electrons with energy in the range 10 to 40 keV, while the specimen is tilted to a large angle, typically 70°. The associated information volume contributing to the formation of the diffraction patterns is compatible with interconnect grain sizes and linewidths, as addressed in more detail in the next section.

We describe in this paper the application of an automated variant of EBSD, termed orientation mapping, as applied to interconnects. Orientation mapping systems consist of computer-controlled beam positioning, diffraction pattern capture and indexing, and software routines for analyzing crystallographic orientation relationships. Included here are examples of analyses carried out on aluminum alloy and copper lines subjected to stress- and electromigration-induced voiding. Emphasis is placed on analysis examples rather than details of the reliability physics, which is

---

\*Partial contribution of the National Institute of Standards and Technology. Not subject to copyright in the U.S.

beyond the scope of this paper. See references (2-4) for such descriptions.

## EXPERIMENTAL CONSIDERATIONS

The basic configuration of an EBSD system as mounted in an SEM is shown in Fig. 1. A phosphor screen affixed to the end of a low-light video system allows the user to view in two dimensions the scattering of electrons from the specimen surface once the stationary beam is positioned in the desired location on the specimen. Typical SEM operating conditions for EBSD characterization include an accelerating voltage in the range 10 to 40 kV, a probe current of approximately 1 nA, and a short working distance. These conditions result in a sufficiently fine probe size while providing a signal-to-noise ratio large enough for accurate pattern indexing.

The information volume contributing to the formation of diffraction patterns is determined by two parameters: (a) the depth into the specimen from which electrons containing orientation information backscatter, and (b) the diameter of the electron probe as resolved on the specimen surface. An upper bound to the orientation-dependent information depth can be given by assuming normal beam incidence on the specimen surface. The Forward-Backward approximation (7), describing the formation of backscattered electron contrast, indicates that orientation-dependent contrast arises from a depth corresponding to approximately two absorption distances into the crystal. The resulting information depths using absorption data from Reimer (8) for 10 to 40 keV electrons in aluminum are approximately 0.06 to 0.12  $\mu\text{m}$ . Analogous depths for copper are 0.03 to 0.05  $\mu\text{m}$ . The penetration in a direction normal to the surface of specimens tilted  $70^\circ$  will be less. The electron probe diameter for a LaB<sub>6</sub> filament operated at 30 kV at a current of 1 nA is approximately 0.02  $\mu\text{m}$  (9) and leads to a resolved spot size of approximately 0.06  $\mu\text{m}$  on the specimen surface. We refer the reader to a recent study of measured versus calculated EBSD spatial resolution, given by Ren *et al.* (10), for further details. The

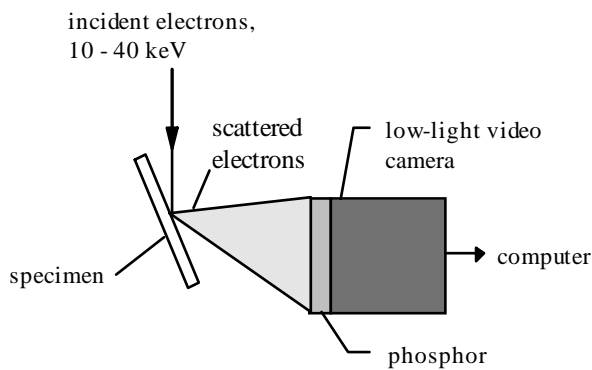


FIGURE 1. Schematic showing specimen and EBSD hardware in the SEM.

total EBSD analysis volume then has a diameter of approximately 0.1  $\mu\text{m}$  or less and is therefore well-suited to the characterization of interconnect structures presently a couple of times larger than that. Much finer spatial resolution can be attained with the use of a field-emission electron source. Present-day instrumentation should be capable of characterizing interconnects with linewidths approaching 0.1  $\mu\text{m}$ , forecasted for manufacture in 2006 (11). With further advances in SEM and EBSD hardware anticipated by that time, we may have a tool that is still applicable to interconnects targeted for manufacture 10 or more years from now.

The EBSD pattern contains an abundance of crystallographic information. Included are the three-dimensional orientation matrix and a semi-quantitative measure of the degree of lattice disorder. A single pattern suffices to assess the orientation matrix since scattering from the specimen occurs divergently and a very large solid angle of scattered electrons is detected. Therefore, all three primary lattice directions contribute to the symmetry of the resulting diffraction pattern. An example of an indexed EBSD pattern obtained from an aluminum alloy is shown in Fig. 2. The bright bands are Kikuchi bands and represent (simplistically) the traces of specific families of atomic planes as they would intersect the phosphor screen. As such, Kikuchi bands act as though rigidly attached to the specimen; hence, tilting the specimen results in translation of the diffraction pattern. Lower index crystallographic zone axes are observed where Kikuchi bands intersect. One possible orientation solution to this particular pattern is shown by the overlaid lines and zone axis indices. Note the large angle of detection, indicated by the fact that poles of both (100) and (110) types are visible. While not 100%

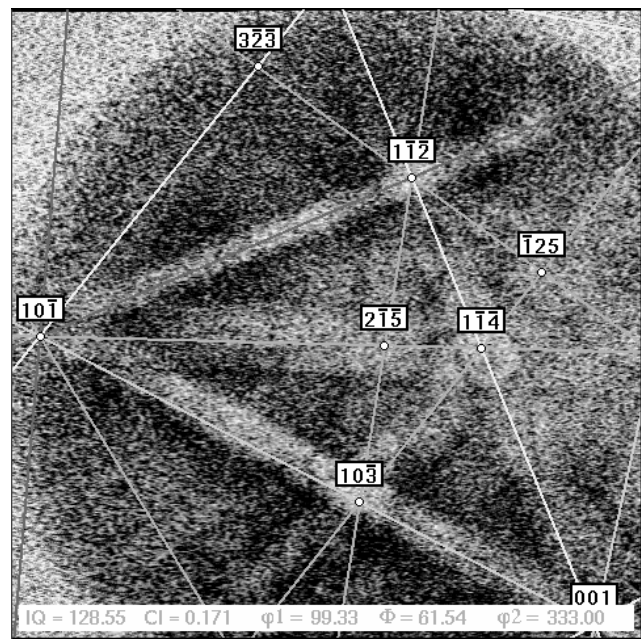


FIGURE 2. Example of indexed EBSD pattern obtained from an aluminum alloy interconnect.

exact, the solutions typically found through the pattern recognition and indexing algorithm are within approximately  $1^\circ$  of the absolute orientation, while relative misorientation determinations can be made to approximately  $0.5^\circ$  (12). The lattice disorder is measured by assessing the degree of diffuseness of the diffraction pattern. More diffuse patterns result upon scattering from a crystal where the lattice disorder is greater, due for instance to a high density of dislocations or point defects, or to disorder associated with a grain boundary.

A specific experimental requirement for EBSD characterization of interconnects is that the specimens must be either unpassivated or de-passivated prior to imaging. An important consideration is to ensure that the underlying metal is left unaltered during de-passivation. This is often done by selective chemical means, either by dissolving the passivating material in an appropriate acid solution or by reactive ion etching. Interconnects without passivating layers are likely to be subjected to stress states significantly different from those of a passivated line, implying that long-term relaxation processes may proceed differently from that expected for a passivated line. A further consequence of exposed interconnects is that the surface will likely react, leading to the thin, native passivating oxide for aluminum or to a more damaging corrosion oxide for copper.

Comprehensive microstructural characterizations are made by collecting a large number EBSD patterns and evaluating them in terms of crystallographic texture. Automated orientation mapping systems are capable of collecting and indexing many thousands of diffraction patterns over a period of several hours. In addition to the obvious spatial resolution advantages, the most significant advantage of orientation mapping over more conventional X-ray diffraction texture measurements centers on the fact that each piece of orientation data can be correlated directly back to the location on the specimen from which the measurement was taken.

### ORIENTATION MAPPING OF INTERCONNECTS

During orientation mapping, the electron beam is moved by a computer system into an array of positions on the specimen surface, and the resulting EBSD pattern corresponding to each position is collected and automatically indexed by means of pattern recognition algorithms. A simple way to display the initial result is to create an image composed of contrast variations that depend on the variations in pattern diffuseness encountered while the beam is rastered across the specimen. Figure 3 shows such an image, obtained from a wide, pure aluminum line, with the beam stepped in  $0.16 \mu\text{m}$  increments. Grain interiors appear brighter, corresponding to sharper EBSD patterns, whereas grain boundary regions



**FIGURE 3.** Orientation map showing grain structure and grain boundaries.

appear darker. Overlaid on this image are bright lines delineating the grain boundaries. This interconnect segment has a polycrystalline grain structure, which is apparent in the image. Such information is normally unavailable through conventional secondary electron imaging or even by channeling contrast during backscattered electron imaging due to the excessive topographic contrast in those imaging modes. Although the spatial resolution available in the image quality map is limited by the EBSD information volume and the distance between beam positions, the user does not have to resort to the less common, and sometimes more tedious, analytical methods of transmission electron microscopy or focused ion beam imaging in order to see the grain structure. Similar analyses from aluminum alloy lines of width  $0.5 \mu\text{m}$  and less have also been reported (13,14).

The same data set used to construct the image in Fig. 3 was used to calculate the crystallographic texture plots in Fig. 4. The orientations displayed in this figure correspond to data taken directly from the single interconnect segment shown above. The  $\langle 111 \rangle$  fiber texture is apparent from these plots. The ability to denote the orientation of specific grains is evident by the orientation map in Fig. 5. Grains are highlighted according to how close their orientations

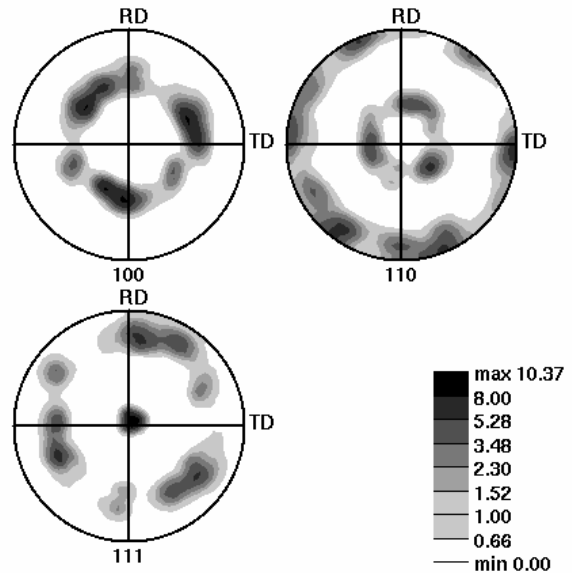


**FIGURE 4.** Pole figures showing predominant  $\langle 111 \rangle$  fiber texture in aluminum interconnect segment. The intensity scale is given in terms of times random. are to the overall average  $\langle 111 \rangle$  fiber texture of the line.



**Figure 5.** Orientation map indicating proximities of grain orientations within  $10^\circ$  of the  $\langle 111 \rangle$  fiber texture. Darker regions are closer to  $\langle 111 \rangle$ .

Darker regions have surface normals most closely aligned with  $\langle 111 \rangle$  directions.

The fact that the relationships between orientation measurements and microstructure are preserved means that we can also infer grain boundary structures to a certain extent. For instance, the distribution of minimum misorientation angles across boundaries is known. With the assumption of perfect columnar grain growth during film deposition, we can assess both the grain boundary plane crystallography and the tilt and twist character associated with any individual boundary. Such information can be useful in describing the diffusive properties of grain boundaries in interconnects. For instance, a local crystallographic characterization of the regions adjacent to stress voids in copper lines (3) revealed that voids formed at triple junctions where three grains intersected with orientations relatively far from the overall average  $\langle 111 \rangle$  fiber texture. Further, the relatively higher misorientation angle boundaries forming voided triple junctions had a significant proportion of twist character to them as well as tilt character with rotation axes parallel to the film plane. Such grain boundary structures are associated with high in-plane diffusivities due to the dislocation structures comprising the boundaries. This suggested that local regions of the interconnect microstructure displaying high in-plane diffusivity were favored sites for significant growth of stress voids.

Orientation mapping has also been used to reveal the grains of damascene-processed lines. Bamboo structures are desired for interconnect structures due to their good resistance to electromigration voiding. Figure 6 shows an orientation map obtained from damascene-processed Al-0.5% Cu lines. The contrast variations indicate how close the grain orientations are to the overall average  $\langle 111 \rangle$  fiber



**Figure 6.** Orientation map showing the near-bamboo grain structure of damascene-processed Al-0.5% Cu lines.

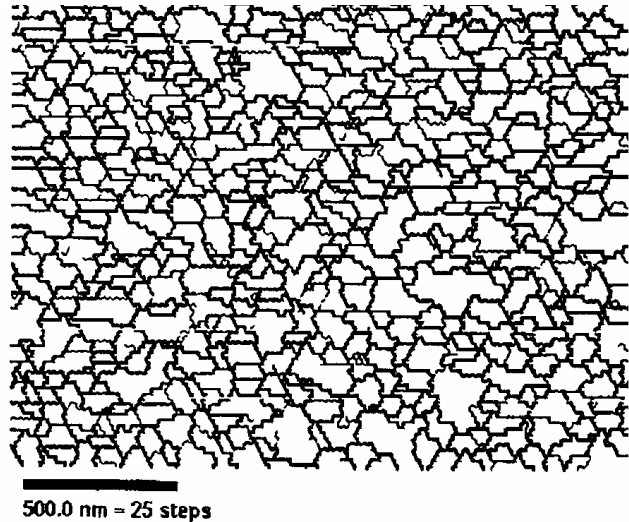


**FIGURE 7.** Orientation map obtained from field emission SEM data, showing grain boundaries in a blanket film of platinum with average grain diameter  $0.075 \mu\text{m}$ . The beam was stepped in  $0.02 \mu\text{m}$  increments. Thinner lines correspond to grain boundaries with misorientation angles less than  $10^\circ$ .

texture. Note that the lines are actually near-bamboo, since several finer grains are visible along the line edges.

The advantages of the spatial resolution of a field emission microscope for orientation mapping are displayed in Fig. 7. Shown is a map displaying the grain boundaries in a blanket film of platinum with average grain diameter  $0.075 \mu\text{m}$ . The data were taken on a SEM with a Schottky source running at an accelerating voltage of 20 kV and a probe current of 1 nA. The beam was stepped in  $0.02 \mu\text{m}$  increments. This result demonstrates that crystallographic orientation mapping with the use of a field emission SEM is capable of revealing grain structure at the sub- $0.1 \mu\text{m}$  level. This characterization method may also be useful for extremely narrow interconnects.

## CONCLUSIONS

Orientation mapping is being used as a measurement tool to aid in the understanding and eventual control of stress voiding and electromigration. These failure mechanisms will become particularly critical as interconnect linewidths decrease and as new material systems such as Cu and low  $k$  dielectrics are introduced (11).

The effects of variables such as local texture and grain boundary misorientations on voiding can be assessed by orientation mapping. This characterization technique will be critical to understanding the interactions among the relevant microstructural variables and their effects on interconnect reliability. The orientation mapping method should find application to future interconnect systems.

## ACKNOWLEDGMENTS

We thank T. N. D. Marieb for providing specimens. We also acknowledge J. A. Nucci for collaborating on the Cu interconnect research and the NIST Office of Microelectronics Programs for support.

## REFERENCES

1. Sheppard, K. G. and Nakahara, S., *Process. Adv. Mater.* **1**, 27-39 (1991).
2. Rodbell, K. P., Hurd, J. L., and DeHaven, P. W., *Mater. Res. Soc. Symp. Proc.* **403**, Pittsburgh: Mater. Res. Soc., 1996, pp. 617-626.
3. Keller, R. R., Nucci, J. A., and Field, D. P., *J. Electron. Mater.* **26**, 996-1001 (1997).
4. Field, D. P. and Dingley, D. J., *J. Electron. Mater.* **25**, 1767-1771 (1996).
5. Field, D. P., *Ultramicros.* **67**, 1-10 (1997).
6. Juul Jensen, D., *Ultramicros.* **67**, 25-34 (1997).
7. Spencer, J. P., Humphreys, C. J., and Hirsch, P. B., *Philos. Mag.* **26**, 193-213 (1972).
8. Reimer, L., *Transmission Electron Microscopy*, New York: Springer-Verlag, 1984, ch. 7, p. 303.
9. Goldstein, J. I., Newbury, D. E., Echlin, P., Joy, D. C., Romig, Jr., A. D., Lyman, C. E., Fiori, C., and Lifshin, E., *Scanning Electron Microscopy and X-Ray Microanalysis*, 2nd ed., New York: Plenum Press, 1992, ch. 2, p. 62.
10. Ren, S. X., Kenik, E. A., Alexander, K. B., and Goyal, A., *Microsc. Microanal.* **4**, 15-22 (1998).
11. *The National Technology Roadmap for Semiconductors: Technology Needs*, 1997 edition, Semiconductor Industry Association, numerous references therein.
12. Dingley, D. J. and Randle, V., *J Mater. Sci.* **27**, 4545-4566 (1992).
13. Hurd, J. L., Rodbell, K. P., Gignac, L. M., Clevenger, L. A., Iggulden, R. C., Schnabel, R. F., Weber, S. J., and Schmidt, N. H., *Appl. Phys. Lett.* **72**, 326-328 (1998).
14. Field, D. P., Sanchez, Jr., J. E., Besser, P. R., and Dingley, D. J., *J. Appl. Phys.* **82**, 2383-2392 (1997).